INDONESIAN JOURNAL ON GEOSCIENCE
Geological Agency
Ministry of Energy and Mineral Resources

Journal homepage: https://ijog.geologi.esdm.go.id
ISSN 2355-9314, e-ISSN 2355-9306

Geotechnical Parameters Determination by Using Seismic Refraction Tomography in The New Capital City of Indonesia, Nusantara: Implication to Analysis of Soil Compaction

Handoyo Handoyo[1], Atika Amalia[1], Asido Saputra Sigalingging[1], Acep Ruchimat[2], Wiyono Wiyono[2], and Özgenç Akin[3]

[1]Geophysical Engineering, Institut Teknologi Sumatera, South Lampung, Indonesia
[2]Pusat Air Tanah dan Geologi Tata Lingkungan, Badan Geologi Bandung, Jawa Barat, Indonesia
[3]Department of Geophysical Engineering, Karadeniz Technical University, Trabzon, Turkey

Corresponding author: handoyo.geoph@tg.itera.ac.id
Manuscript received: April, 14, 2025; revised: July, 03, 2025;
approved: October, 05, 2025; available online: November ,17, 2025

Abstract - The new capital city of Indonesia, Nusantara, in East Kalimantan, is undergoing enormous infrastructural development in Indonesia. Understanding the condition of the soil, sediment, and hardrock layers at this location is critical for geotechnical working principles. In this study, the first arrival P-wave tomography method was used to determine the distribution of P-wave velocity and geotechnical parameters (*e.g.* porosity, density, void ratio) to better understand the condition of the rock layers at this location. This study involved the use of seismic refraction tomography data consisting of forty-eight channels with a distance between geophones of 1 m, and a source in the form of a sledgehammer weighing 3 kg with a separation distance of 3 m. The natural frequency of the geophones used was 4.5 Hz with a recording time of 1.0 sec. Results of this investigation reveal a thinning hardrock layer from the south to the north, with a thickness ranging from 7 to 16 m correlated to consolidated alluvium. Moreover, the geotechnical parameter of sediment layers, top soil (clayey soil) and unconsolidated alluvium, has a density value range from 1.6 to 1.8 g/cm^3, porosity 0.31 to 0.38, and void ratio 0.44 to 0.59. These findings show that the soil layer in the south to the middle of line profile of the studied area has low to medium compaction, requiring soil hardening activities (mechanical compaction) for infrastructure construction. Finally, the findings of this study are expected to help with infrastructure development in the IKN by utilizing geophysical technique.

Keywords: IKN, Nusantara, seismic, tomography, geotechnic, hardrock

How to cite this article:
Handoyo, H., Amalia, A., Sigalingging, A.S., Ruchimat, A., Wiyono, W., and Akin, Ö,. 2025. Geotechnical Parameters Determination by Using Seismic Refraction Tomography in The New Capital City of Indonesia, Nusantara: Implication to Analysis of Soil Compaction. *Indonesian Journal on Geoscience*, 12 (3), p.423-435. DOI:10.17014/ ijog.12.3.423-435

Introduction

Background

Nusantara, the Indonesia new capital city, is still developing its infrastructure in several areas, including buildings and highway construction. For geotechnical applications, such as the construction of pavements and foundations in civil engineering, information about soil thickness and the depth of hard rock is required. Thus, the depth of the hardrock layer, the thickness of the soil layer, and the sediment layer may all be determined with the aid of geophysical techniques. Information on geotechnical parameters (*e.g.* hardrock, porosity, density, and void ratio) that can aid in the infrastructure development process can also

be derived by the geophysical method (Pegah and Liu, 2016; Nabil and Ahmed, 2014; Butchibabu *et al*., 2023; Qaher *et al*., 2023; Cichostępski *et al*., 2024; Chevva, 2025).

Seismic refraction tomography (SRT) is a geophysical technique that determines a velocity depth model (2D/3D) by using inversion techniques to interpret seismic refraction data (White, 1989; Zelt and Barton, 1998; Bery, 2022). Geotechnical parameters such as density, porosity, and void ratio are often obtained directly from sample tests from excavations or drilling data. However, the information covers limited dimensions, usually vertically (1-dimension), therefore geophysical methods (seismic refraction tomography) are expected to be able to model these geotechnical parameters laterally. Based on the tomography concept, an object is divided into cells known as voxels in three dimensions and pixels in two dimensions (Epili *et al*., 2001; Noori *et al.*, 2012; Capizzi *et al*., 2025; Cheng *et al*., 2025). Instead of describing the velocity as layers, profiles can be used to identify the velocity distribution in an object using tomographic imaging (Criss *et al*., 2001; Fernández-Baniela *et al*., 2021; Pegah, 2025). The travel-time durations of an initial model, which needs to be made before the inversion starts, are iteratively calculated and compared with the actual data using this inversion method. Then, the original model is altered to reduce the difference between the computed and actual travel-time (Epili *et al*., 1999; Rawlinson and Spakman, 2016; Tsai *et al*., 2023; Torres *et al*., 2024).

This study aims to determine: (i) the depth of the hardrock layer; (ii) the distribution of density values; (iii) the distribution of porosity values; and (iv) variations in void ratio values. This study also aims to describe the distribution of these geotechnical parameters using geophysical methods, thereby contributing to the feasibility study for infrastructure development in the new capital city, Nusantara.

Geological And Stratigraphical Settings

Stratigraphically, East Kalimantan is dominated by Tertiary to Quaternary sedimentary deposits consisting of sandstone, mudstone, shale, and limestone. There are several formations in this area, including The Balikpapan Formation (Tmbp), Belulu Formation (Tmbl), Alluvial deposits (Qa), Kampungbaru Formation (Tpkb), Palaubalang Formation (Tmpb), Pamaluan Formation (Tomp), and Tuyu Formation (Toty), which are generally composed of clastic rocks resulting from sedimentation in deltaic to shallow sea environments (Hidayat and Umar, 1994). At the near surface (Qa-aged rock formation layer), it consists of several lithologies of gravel, pebbles, sand, clay, and mud which are the result of sedimentation processes formed in fluvial, swampy, coastal, and deltaic environments. These deposits are widespread along the eastern coastal area of Tanah Grogot, as well as in The Adang Bay and Balikpapan Bay areas.

This study was conducted in the North Penajam Paser Regency, East Kalimantan (Figure 1), where the measurement coordinates are shown in red rectangle, and the area is included in the alluvium formation. The alluvium formation consists of gravel, pebbles, sand, and mud as river, swamp, and delta deposits spread along the east coast of Tanah Grogot, Adang Bay, and Balikpapan Bay. In addition to The Alluvium Formation, there are also The Kampungbaru Formation, The Pamaluan Formation, and The Balikpapan Formation (Supriatna *et al*., 1995; Clay *et al*., 2000).

Methods and Materials

Materials

Seismic refraction data were acquired at a proposed road crossing site to connect the port and toll road near the Nusantara area. The survey aimed to capture the first arrivals of direct and refracted P-waves. The acquisition setup included forty-eight vertical geophones with a 4.5 Hz natural frequency, spaced at 1 m intervals along a linear profile. A 3 kg sledgehammer was used as the seismic source, with shot points positioned every 3 m. Data were recorded over a duration of 1.0 sec. with a sampling interval of 1 millisecond.

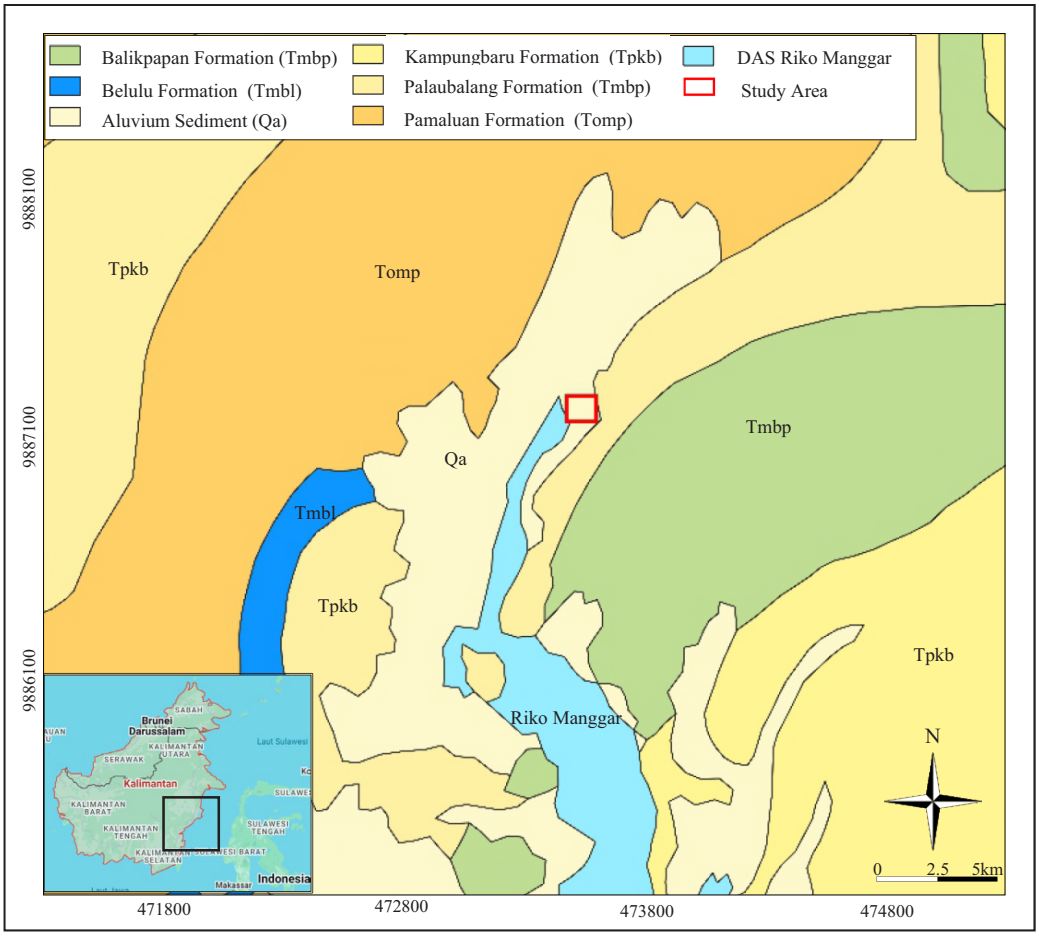

Figure 1. Geological map of the studied area, East Kalimantan (modified from Hidayat and Umar, 1994; Supriatna *et al*., 1995; Clay *et al*., 2000).

The survey line was established on relatively flat terrain, with no significant topographic variation observed along the profile. Moreover, this research is also equipped with lithology sample data around the researched location using a bore hand drill.

Method

The methods used in this study are: (i) *Vp* velocity inversion from the first arrival P-wave tomography technique or seismic refraction tomography; (ii) Hardrock interpretation from the determination of the *Vp* depth model; (iii) Density estimation from the *VP* depth profile; (iv) Porosity estimation from density; and (v) Void ratio estimation from the porosity profile.

First, for resolving the *Vp* velocity structure, P-wave travel time tomography has become a popular and well-established inversion approach (Aki and Richards, 1980; Nolet, 1993; Thurber and Atre, 1993). By minimizing the time difference between the predicted travel time, the general method employs the first-arrival travel time to find the optimum velocity model that can replicate the observed ones. Thus, a ray-tracing forward modeling approach is used to compute theoretical travel time. The Delta-T-v inversion method (Rohdewald, 2011) was employed to derive the subsurface velocity distribution from the selected travel time by the first arrivals. The Common Midpoint (CMP) refraction theory (Gebrande and Miller, 1985) is the basic idea of this method. It postulates that the CMP travel-time can be understood as functions of the independent variables CMPx coordinates and the CMP constant offset. The reciprocal apparent CMP velocities are then obtained by two partial differentiations. With the advantage of not requiring extrapolation to the

shot sites, this method is conceptually comparable to forward and backward shot analysis. Instead, it uses the local layer thickness H(X), which is determined at each CMP. The refractor is a circular enclosure with a radius that surrounds the surface of the CMP.

The second stage is the interpretation of the hardrock layer from the Vp depth model. Top soil, soil, and sediment layers generally have low velocities. While hardrock has a higher velocity, usually ranging from more than 1,300m/s (Mills, 1990; Babacan *et al*., 2018; Handoyo *et al*., 2022). After the interpretation of the depth of the hardrock layer was obtained, the third stage was to predict the density value (ρ). Simply, the density value could be predicted using the P-wave velocity value (*VP*), which is written in Equation 1 (Gardner *et al*., 1974). Density is a physical parameter that shows the density value of a rock layer, meaning the greater the value, the denser and more compact the layer (Waddell *et al*., 2010; Kodikara *et al*., 2018).

$$\rho = 0.31 V_P^{0.25} \quad \text{..... (1)}$$

The next stage is the prediction of porosity value. Porosity in geotechnics shows the value of a layer of soil or sediment whether it is compact or not. The greater the porosity value, the less compact the layer is. Mathematically, porosity (Φ) can be predicted using the density value as shown in Equation 2, where ρ_{ma} is the density of quartz (2.65 g/cm³) and ρ_f density of water (1 g/cm³) that assumed the layers were saturated by water.

$$\varnothing = \frac{\rho_{ma} - \rho}{\rho_{ma} - \rho_f} \quad \text{..... (2)}$$

The last stage in this study is void ratio prediction. In geotechnical engineering, void ratio is the ratio of the volume of voids (V_V) in soil to the volume of solids (V_S), illustrated in Figure 2. It is a measure of the fractional volume of soil pores. Mathematically, the void ratio value (*e*) can be predicted using the porosity value as shown in Equation 3. The sediment layer becomes less compact as the void ratio value increases (Tarantino and De Col, 2008; Shi and Zhao, 2020).

$$e = \frac{V_v}{V_s} = \frac{\theta}{1-\theta} \quad \text{..... (3)}$$

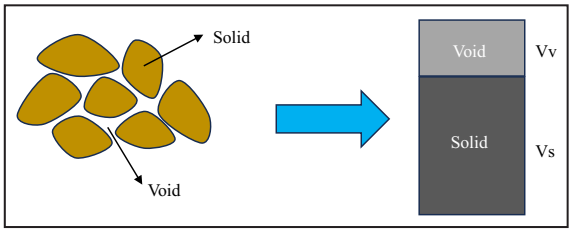

Figure 2. Illustration of void ratio in geotechnic (modified from Shi and Zhao, 2020; Tarantino and De Col, 2008).

Result and Analysis

Vp Depth Profile from Seismic Refraction Tomography

The SeisImager package handles a number of the software utilized in this investigation. The raw data of seismic recordings has undergone several standard stages in seismic refraction tomography, such as adding gain to strengthen the signal and amplitude normalization to provide better seismic resolution. Examples of the results of adding gain and amplitude normalization are shown in Figure 3a, Figure 3b, and Figure 3c. The main purpose of this stage is to provide clear image resolution of the trends of direct and refracted waves. In Figure 3a, the direct wave is identified by the blue trend line which starts to be detected at arrival time around 20-23 ms and the refraction wave appears from time 24-50 ms at the last geophone. Then, in Figure 3b, a pair of direct wave trends centred in the middle and detected at time 0-20 ms. Meanwhile, refraction waves are identified at time 22-40 ms on the left side of the shot point and 20-40 ms on the right side. In Figure 3c, the direct wave was detected at arrival time around 24-30 ms and the refraction wave appears from time 30-55 ms.

The next stage is picking the first arrival P- wave travel-time. The first arrival time for the recorded P-wave data was manually picked. Noise monitoring and robust geophone coupling

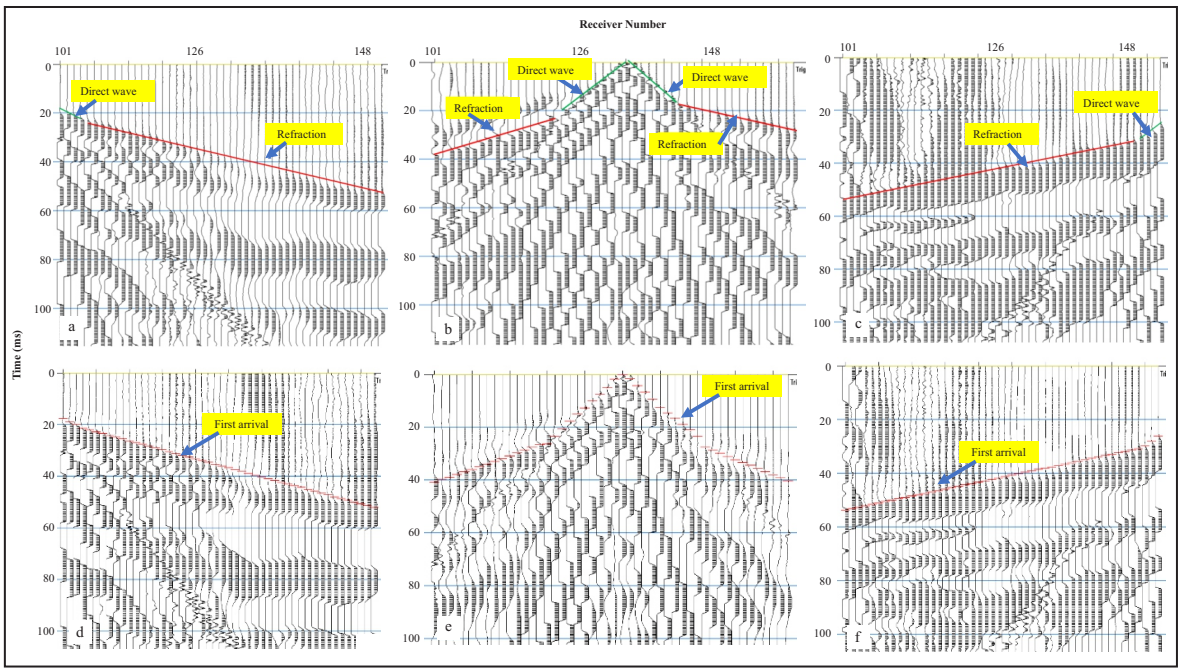

Figure 3. a-c) Seismic direct and refraction identification. d) Picked first arrival travel-time from 2a. e) Picked first arrival travel-time from 2b. f) Picked first arrival first arrival from 2c.

were among the quality control measures utilized during the data collection to achieve a high signal-to-noise ratio in the shot records. As a result, consistent picking was feasible with the acquired shots. Bad traces and noise were deleted to prevent misleading shots. To ensure correctness, the first arrivals were checked and validated at regular intervals. Several first breaks in this study were selected, and then used for travel-time tomography (Figures 3d-3f).

Two steps are required to determine the combined velocity field for a multishooting geometry: superposition of the velocity functions computed for various pairs of traveltime curves and an accurate solution of the inverse problem, which is to determine an increasing homogeneous function from two reversed travel-time curves of first arrivals (Piip and Efimova, 1996; Piip and Naumov, 2004). Next, velocity values are calculated at various positions on a rectangular grid (the grid representation) were used to depict the final velocity section. The initial model for the final tomographic inversion was constructed using information from the resultant models, such as the minimum and maximum velocity, number of layers, and depth to the lowest layers (Figure 4b).

Through iterations, the residuals (the discrepancies between calculated and observed travel-time) were minimized in order to improve the original model. The least square approach is usually used to do this minimization. At least ten iterations are selected and an ideal fit between the measured and calculated travel-time is indicated by an estimated RMS error of 1 to 4 ms or RMS error <5 % (Figure 4a). The raytracing procedure in the Plotrefa software was used to verify the consistency between the model and the data to improve the understanding of the models. The penetration of the seismic rays used to compute the synthetic travel-times in the tomographic inversion can be estimated via forward modeling (Leung, 1997; Sheehan *et al.*, 2005).

Hardrock and Soil Layer Interpretation

A primary objective of generating the Vp depth profile is to estimate a hardrock depth based on characteristic Vp velocity values. In this study (Figure 5), the lowest Vp < 900 m/s at the first depth of 2 to 2.5 m near the surface was correlated with top soil (clayey soil) with low velocity characteristics caused by low bulk modulus and stiffness (Williams *et al.*, 2003; Uyanik, 2010). As a control, bore data

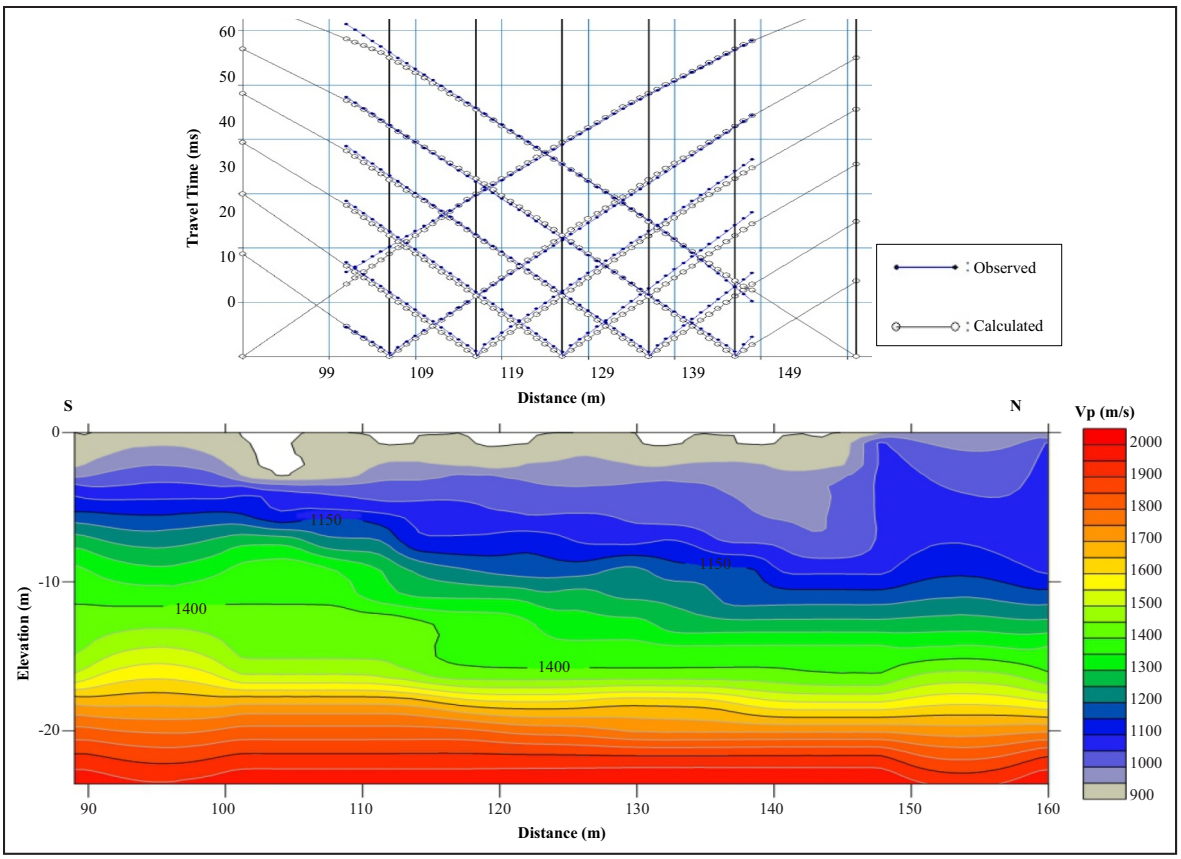

Figure 4. a) Examples of the traveltime-distance curves of the survey. b) Vp depth profile from inversion.

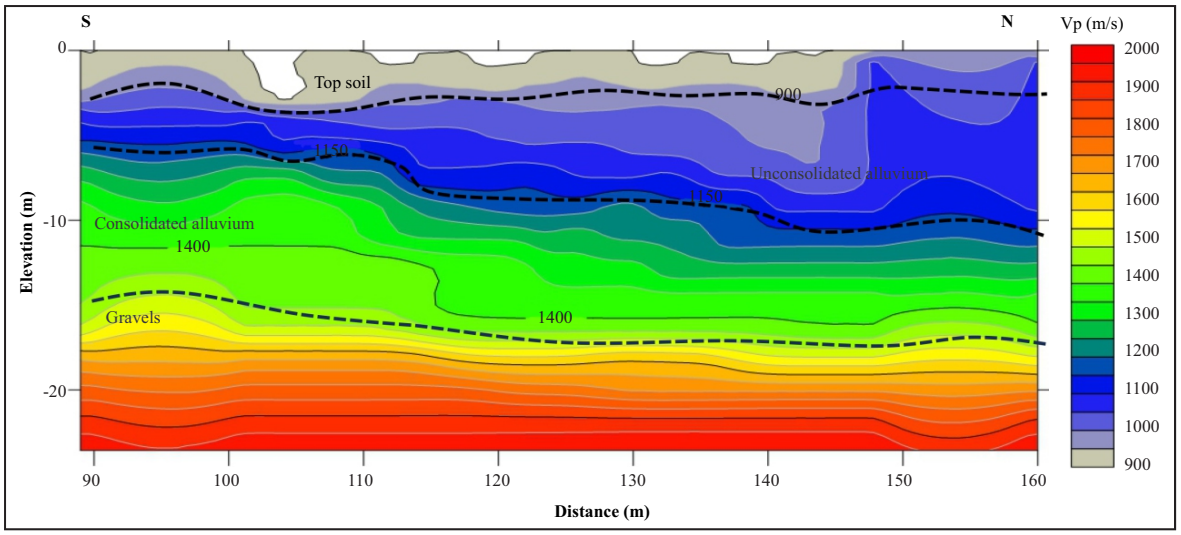

Figure 5. The interpretation of several layers from Vp depth profile.

near the seismic line showed corresponding results in the form of clay and silt sediments (Figure 6). Thus, the top soil (clayey soil) at this location is correlated with clay and silty clay with characteristics of soft to medium stiffness, low to medium plasticity and a little sand in the deepest layer. The second layer, the higher Vp velocity 900-1200 m/s interpreted as a dense soil with lithology from bore data (Figure 6) consists of silt with slightly clayey, stiff to very stiff, and medium plasticity that corre-

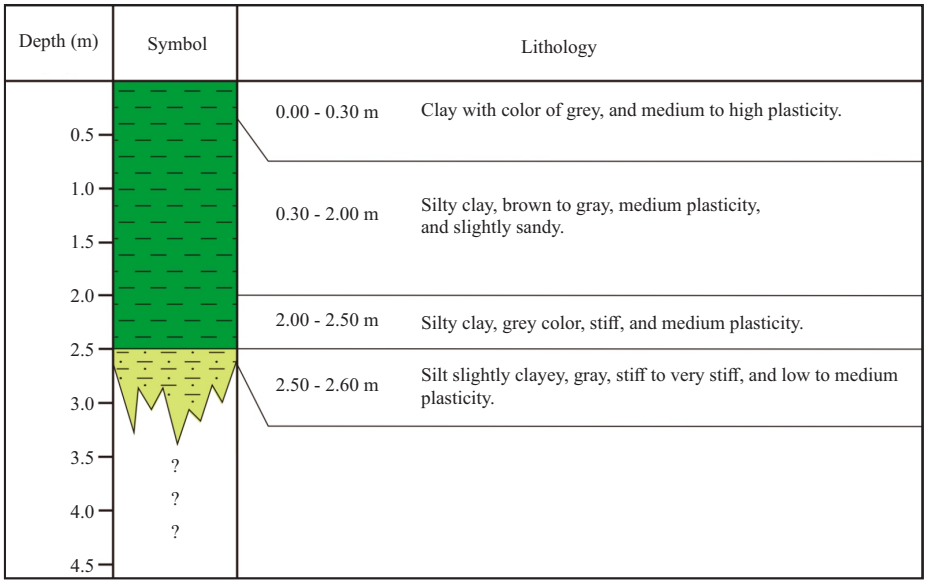

Figure 6. The bore data in studied area with maximum penetration depth of about 3.5 m.

lated unconsolidated alluvial sediment (Carvalho *et al*., 2009; Uyanik, 2010). The thickness of this layer ranges from 2.5 to 7 m in the south and thickens to 2 to 11 m in the north.

Then, Vp velocity at a value of 1,200-1,400 m/s is interpreted as a hardrock layer that correlates with the consolidated alluvium layer in The Alluvium Formation. The consolidated alluvium layer can be in the form of sand lithology, which generally consists of primary material in the form of medium to coarse sand grains, and has a medium to dense density level (Mills, 1990; Von Voigtlander *et al*., 2018; Babacan *et al*., 2018; Handoyo *et al*., 2022). This layer is at a depth of 7-15 m on the south side, and thins to 11-16 m on the north side of the track. Finally, for Vp velocity >1,400 m/s it is interpreted as a layer with gravel consisting of main material in the form of medium to dense gravel at the depth of 15 m on the south side, and deepens to a depth of 17 m on the north side.

Determination of Geotechnical Parameters

The geotechnical parameters-density, porosity, and void ratio-were evaluated to characterize subsurface materials. First, density values (Figure 7), calculated using the Gardner Equation, range from 1.68 to 1.76 g/cm³ in top soil (clayey soil) and exceed 1.9 g/cm³ in gravels. Next, porosity values (Figure 8), derived from Equation 2, are highest (>0.35) in top soil (clayey soil) and drop below 0.27 in gravels. Finally, the void ratio (Figure 9), calculated from porosity, is greater than 0.55 in top soil (clayey soil) and less than 0.39 in gravels. All units and value ranges have been standardized for clarity.

Discussion

Soil Compaction Analysis from Geotechnical Parameters

Compaction has a strong impact on important processes occurring in the soil, such as the circulation of water, air, heat, and nutrients as well as the strength of the soil to support infrastructure development such as buildings and roads (Arvidsson, 1999; Défossez *et al*., 2003). The process of mechanically raising soil density is known as soil compaction. This is an important step in the building process in construction. Inadequate execution may cause soil settlement, which could lead to needless maintenance expenses or structural failure. Mechanical compaction techniques are used in practically every kind of construction site and project.

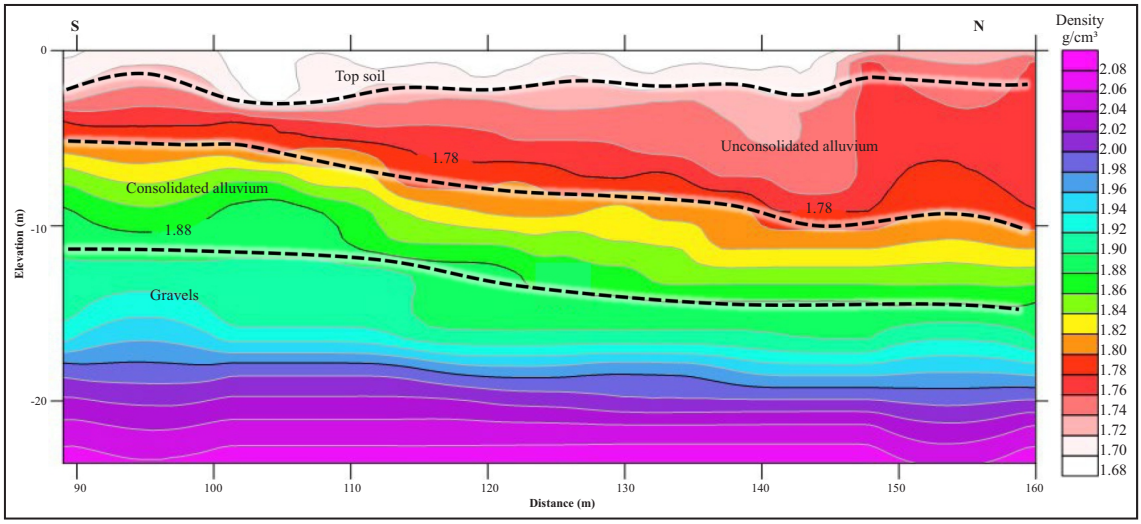

Figure 7. The distribution of density value. Density of hardrock layer starts from 1.8 g/cm³ and above.

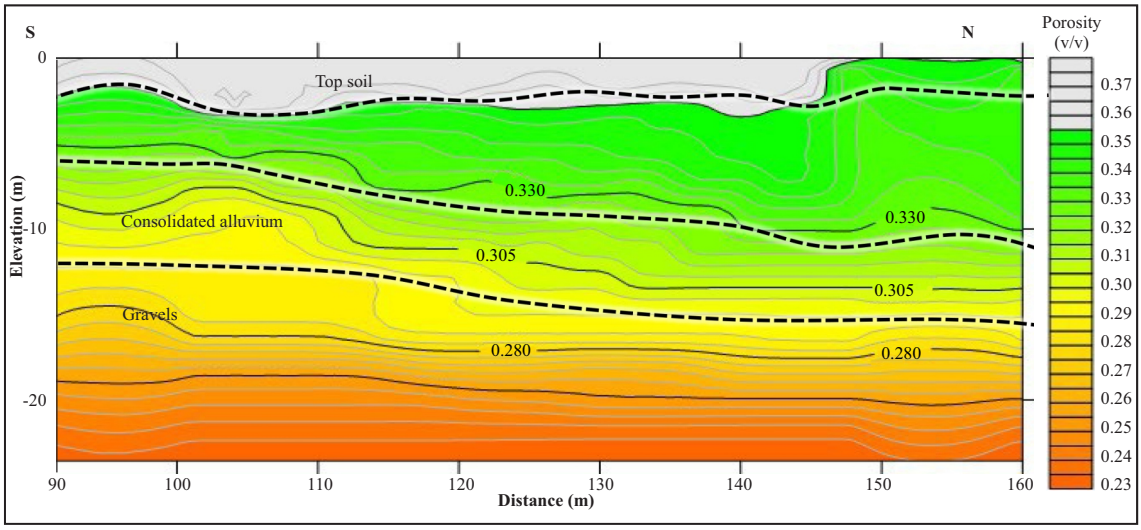

Figure 8. The distribution of porosity value. Porosity of a hardrock layer interpreyed lower than 0.3 or <30 %.

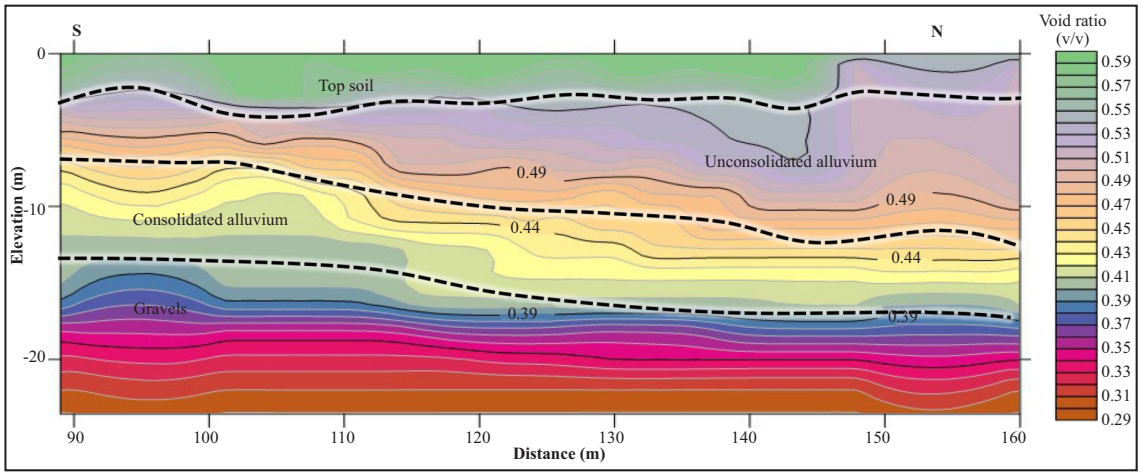

Figure 9. The distribution of void ratio. Void ratio of a hardrock layer estimated lower than 0.45.

During compaction, it is critical to understand and regulate the soil density. The common field tests listed below can be used to instantly ascertain whether compaction densities are being reached. Density is one of the physical parameters (seismic properties together with Vp velocity) which plays a role in determining the degree of compaction of a sediment layer (Waddell *et al.*, 2010; Kodikara *et al.*, 2018). In Figure 10, the density distribution of the top soil (clayey soil) layer varies with a density interval of 1.68-1.76 g/cm³, which means it shows different degrees of compaction. The top soil (clayey soil) layer on the north side has a higher density (~1.76 g/cm³) than the south-middle side of the track (~1.68 g/cm³), which means the top soil (clayey soil) on the north side is relatively more compact (compacted soil or improved load support) compared to the south-middle of line profile. Thus, the top soil (clayey soil) layer on the south-middle of line profile (loose soil or poor load support) requires more intense mechanical compaction treatment.

The identical behaviour is also shown by the distribution of porosity and void ratio values. In Figure 7 and Figure 8, the north side of the line profile has a porosity value of ~0.34 and void ratio value of ~0.50 that is smaller than the south-middle side, which means that the percentage of void space (pores) in this area is less than the solid phase. The less space between solid grains correlated to the higher the degree of compaction of the sediment (Shi and Zhao, 2020)

Limitation of This Study

The geophysical method is an indirect approach used to predict the distribution of sediment layers below the surface. In this study, the seismic refraction tomography method has been applied on a single track with the aim of producing rapid initial information about the subsurface conditions at the studied site (where the data processing on seismic refraction is relatively short). However, bore or excavation data is the key to the success of estimating subsurface conditions. Therefore, in this study, information on bore is needed for more deeper penetration to validate predictions obtained from the geophysical approach, where the bore data available in this study is relatively shallow with a depth of <5 m.

Another alternative can be done by approaching several geophysical methods. In this case, subsurface profiling from Vp velocity data can be combined with data from V_S velocity. According to several earlier researches, Vp and V_S velocity profiles together can yield more appropriate interpretation results (Uyanik, 2020; Handoyo *et al.*, 2022; Flinchum *et al.*, 2024). In the next study, the Multichannel Analysis of Surface Waves (MASW) method will be applied to help estimate

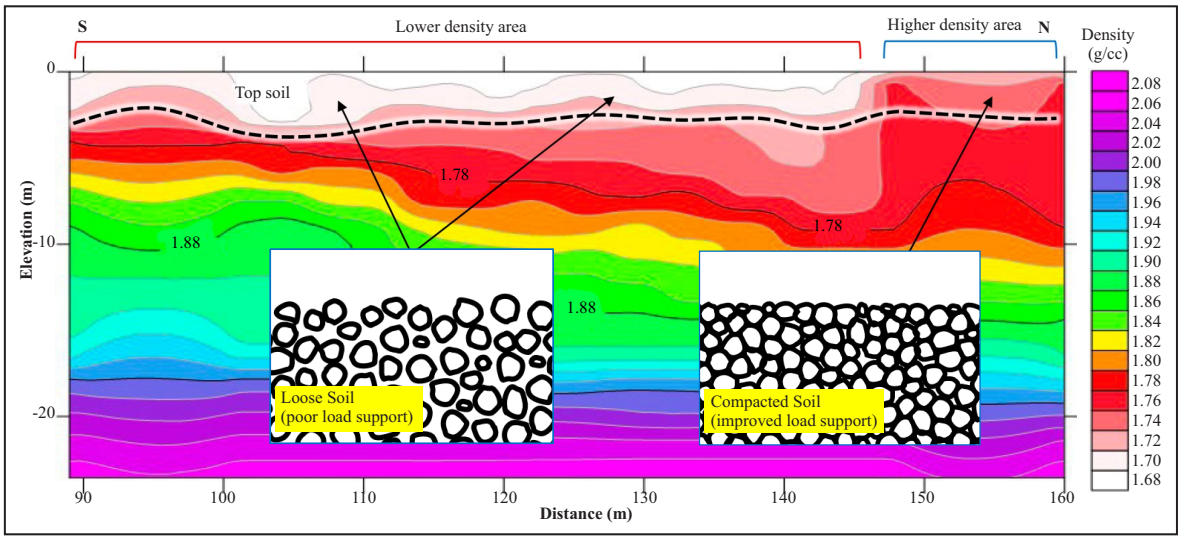

Figure 10. Correlation between density and compactness of a sediment layer.

subsurface conditions more accurately. By combining several geophysical methods, it is hoped that the error values obtained can be minimized to provide more relevant results.

Conclusions

Information on the compactness of a soil layer is crucial in infrastructure development, both buildings and highways. The degree of compaction of a soil layer can be predicted using geotechnical parameters which in this study are derived from geophysical parameters (seismic wave velocity). Seismic refraction tomography was employed to map the distribution of Vp velocity, and then transformed it into geotechnical parameter profiles including density, porosity, and void ratio. By using this method, this information has been obtained more quickly and effectively.

The results of this study show that the thickness of the top soil (clayey soil) layer along the path is relatively parallel to the surface with a thickness variation of 2-3 m and a hardrock depth of 7-15 m from the surface. On the north side of the measurement path, it was detected to have a higher density value (~1.76 g/cm^3), lower porosity (~0.34), and a lower void ratio (~0.5), which means it has a higher degree of compaction than the south-middle line profile. As an implication, the south-middle side requires an intensive mechanical compaction process. These findings demonstrate the potential of seismic refraction tomography as a reliable and efficient tool for assessing soil compaction and for supporting informed decision-making in infrastructure development.

Acknowledgments

The author thanks The Geological Agency, Pusat Air Tanah dan Geologi Tata Lingkungan, Badan Geologi Bandung, for permission to use the data in this study. This research was funded by LPPM Institut Teknologi Sumatera, grant number 1539j/IT9.2.1/PT.07.03/2025.

References

Aki, K. and Richards, P.G., 1980. *Quantitative seismology: Theory and methods,* 1. San Francisco, W.H. Freeman and Company. 932pp.

Arvidsson, J., 1999. Nutrient uptake and growth of barley as affected by soil compaction. *Plant and soil,* 208, p.9-19.

Babacan, A.E., Gelisli, K., and Tweeton, D., 2018. Refraction and amplitude attenuation tomography for bedrock characterization: Trabzon case (Turkey). *Engineering Geology,* 245, p.344-355. DOI: 10.1016/j.enggeo.2018.09.008.

Bery, A.A., 2022. Development of Soil Cohesion and Friction Angle Models Using Multiple Linear Regression (MLR) Statistical Techniques. *Indonesian Journal on Geoscience*, 10 (1), p.15-25. DOI: 10.17014/ijog.10.1.15-25

Butchibabu, B., Jha, P.C., Sandeep, N., and Sivaram, Y.V., 2023. Seismic refraction tomography using underwater and land based seismic data for evaluation of foundation of civil structures. *Journal of Applied Geophysics,* 210, 104934. DOI: 10.1016/j.jappgeo.2023.104934.

Capizzi, P., Carollo, A., Martorana, R., and Pirrera, C., 2025. Cluster Analysis of 3D SRT and ERT in Urban Environment: Cavity Detection in Agrigento (Italy). *NSG 2025, 31st Meeting of Environmental and Engineering Geophysics,* 2025 (1), p.1-5. European Association of Geoscientists and Engineers. DOI: 10.3997/2214-4609.202520132.

Carvalho, J., Torres, L., Castro, R., Dias, R., and Mendes-Victor, L., 2009. Seismic velocities and geotechnical data applied to the soil microzoning of western Algarve, Portugal. *Journal of Applied Geophysics*, 68 (2), p.249-258. DOI: 10.1016/j.jappgeo.2009.01.001.

Cichostępski, K., Dec, J., Golonka, J., and Waśkowska, A., 2024. Shallow seismic refraction tomography images from the pieniny klippen belt (Southern Poland). *Minerals*, 14 (2), 155p. DOI: 10.3390/min14020155.

Cheng, N., Ismail, M.A.M., Muztaza, N.M., Pauzi, F.N.A., Zakaria, M.T., and Yokota, Y., 2025. From 2-D seismic refraction to 3-D

subsurface characterization: Unpacking the role of univariate spatial interpolation techniques with borehole validation. *Physics and Chemistry of the Earth,* Parts A/B/C, 104113. DOI: 10.1016/j.pce.2025.104113.

Chevva, K., 2025. Near-Surface Geophysical Techniques for Addressing Geotechnical Problems. *Indian Geotechnical Journal*, p.1-22. DOI: 10.1007/s40098-025-01372-7.

Clay, K.Mc., Dooley, T., Ferguson, A., and Poblet, J., 2000. Tectonic evolution of the Sanga Sanga Block, Mahakam Delta, Kalimantan, Indonesia. *AAPG Bulletin,* 84, p.765-786.

Criss, J., Epili, D., and Cunningham, D., 2001. Turning-Ray Tomography for Statics Solution. *63rd EAGE Conference and Exhibition* (pp. cp-15). European Association of Geoscientists and Engineers.

Défossez, P., Richard, G., Boizard, H., and O'Sullivan, M.F., 2003. Modeling change in soil compaction due to agricultural traffic as function of soil water content. *Geoderma,* 116 (1), p.89-105. DOI: 10.1016/S0016-7061(03)00096-X.

Epili, D., Neff, W.H., and Grieger, J.C., 1999. 3-D WARRP design for exploration targets. *SEG Technical Program Expanded Abstracts*, p.985-988. Society of Exploration Geophysicists.

Epili, D., Criss, J., and Cunningham, D., 2001. Turning-ray tomography for statics solution. *SEG International Exposition and Annual Meeting (pp. SEG-2001)*.

Fernández-Baniela, F., Arias, D., and Rubio-Ordóñez, Á., 2021. Seismic refraction and electrical resistivity tomographies for geotechnical site characterization of two water reservoirs (El Hierro, Spain). *Near Surface Geophysics,* 19 (2), p.199-223. DOI: 10.1002/nsg.12152.

Flinchum, B.A., Grana, D., Carr, B.J., Ravichandran, N., Eppinger, B., and Holbrook, W.S., 2024. Low Vp/Vs values as an indicator for fractures in the critical zone. *Geophysical Research Letters,* 51 (2), e2023GL105946. DOI: 10.1029/2023GL105946.

Gardner, G.H.F., Gardner, L.W., and Gregory, A., 1974. Formation velocity and density-The diagnostic basics for stratigraphic traps. *Geophysics,* 39 (6), p.770-780.

Gebrande, H. and Miller, H., 1985. Refraktionsseismik. *Angewandte Geowissenschaften,* II, p.226-260.

Handoyo, H., Defelipe, I., Martín-Banda, R., García-Mayordomo, J., Martí, D., MartínezDíaz, J.J., Insua-Ar´evalo, J.M., Teixido, ´ T., Alcalde, J., Palomeras, I., and Carbonell, R., 2022. Characterization of the shallow subsurface structure across the Carrascoy Fault System (SE Iberian Peninsula) using P-wave tomography and Multichannel Analysis of Surface Waves. *Geology Acta,* 20 (9), p.1-19. DOI: 10.1344/GeologicaActayear.volume.manuscript.

Hidayat, S. and Umar, I., 1994. *Peta Geologi Regional Lembar Balikpapan, Kalimantan skala 1:250.000.* Pusat Penelitian dan Pengembangan Geologi, Bandung.

Kodikara, J., Islam, T., and Sounthararajah, A., 2018. Review of soil compaction: History and recent developments. *Transportation Geotechnics,* 17, p.24-34. DOI: 10.1016/j.trgeo.2018.09.006.

Leung, T.M., 1997. Evaluation of seismic refraction interpretation using first arrival raytracing. Geological Society, London. *Engineering Geology Special Publications,* 12 (1), p.413-416.

Mills, H.H., 1990. Thickness and character of regolith on mountain slopes in the vicinity of Mountain Lake, Virginia, as indicated by seismic refraction, and implications for hillslope evolution. *Geomorphology,* 3 (2), p.143-157.

Nabil, H.A.S. and Ahmed, J.H., 2014. Seismic Refraction Tomography and MASW Survey for Geotechnical Evaluation of soil for the Teaching Hospital Project at Mosul University. Sulaimani *Journal for Pure and Applied Sciences,* 16 (1), p1-14. DOI: 10.17656/jzs.10279.

Nolet, G., 1993. Solving large linearized tomographic problems. In: Iyer, H.M., Hirahara, K. (eds.). *Seismic Tomography, theory and practice.* London, Chapman and Hall, p.227-247.

Noori, M., Shadizadeh, S.R., Riahi, M.A., and Jamali, J., 2012. The effect of initial velocity model accuracy on refraction tomography velocity model in Sefid-Zakhor gas field, Iran. *Journal of American Science,* 8 (9). DOI: 10.7537/marsjas080912.71.

Pegah, E. and Liu, H., 2016. Application of near-surface seismic refraction tomography and multichannel analysis of surface waves for geotechnical site characterizations: A case study. *Engineering Geology,* 208, p.100-113. DOI: 10.1016/j.enggeo.2016.04.021.

Pegah, E., 2025. Evaluation of Transversely Isotropic Elastic Parameters of Natural Soils through the Combined Use of Seismic Refraction and Downhole techniques. *Journal of Engineering Geology,* 19 (1), 2pp. DOI: 10.22034/JEG.2025.19.1.1019164.

Piip, V.B. and Efimova, E.A., 1996. *Investigation of the deep structure of the Eastern European Platform using seismic refraction data*.

Piip, V.B. and Naumov, A.N., 2004. Refraction and CDP reflection shallow seismics for detection of low amplitude faults. *66th EAGE Conference and Exhibition (pp. cp-3)*. European Association of Geoscientists and Engineers. DOI: 10.3997/2214-4609-pdb.3.P146.

Qaher, M., Eldosouky, A.M., Saada, S.A., and Basheer, A.A., 2023. Assessing Geotechnical Property for Construction Purposes: A Study on the Efficacy of Shallow Seismic Refraction Tomography Method. *Frontiers in Scientific Research and Technology,* 7 (1). DOI: 10.21608/fsrt.2023.229137.1102.

Rawlinson, N. and Spakman, W., 2016. On the use of sensitivity tests in seismic tomography. *Geophysical Journal International,* 205 (2), p.1221-1243. DOI: 10.1093/gji/ggw084.

Ren, L., Cornelis, W.M., Ruysschaert, G., De Pue, J., Lootens, P., and D'Hose, T., 2022. Quantifying the impact of induced top soil and historical subsoil compaction as well as the persistence of subsoiling. *Geoderma,* 424, 116024. DOI: 10.1016/j.geoderma.2022.116024.

Richer-de-Forges, A. C., Arrouays, D., Libohova, Z., Chen, S., Beaudette, D.E., and Bourennane, H., 2024. Revealing Top soil Behavior to Compaction from Mining Field Observations. *Land,* 13 (7), 909. DOI: 10.3390/land13070909.

Rohdewald, S.R., 2011. Interpretation of First-Arrival Travel Times with Wavepath Eikonal Traveltime Inversion and Wavefront Refraction Method. *Symposium on the Application of Geophysics to Engineering and Environmental. Problems Proceedings*, p.31-38. DOI: 10.4133/1.3614086.

Sheehan, J.R., Doll, W.E., Watson, D.B., and Mandell, W.A., 2005. Application of seismic refraction tomography to karst cavities. *US geological survey karst interest group proceedings*, Rapid City, South Dakota, p.29-38.

Shi, X.S. and Zhao, J., 2020. Practical estimation of compression behavior of clayey/silty sands using equivalent void-ratio concept. *Journal of Geotechnical and Geoenvironmental Engineering,* 146 (6), 04020046. DOI: 10.1061/(ASCE)GT.1943-5606.0002267.

Supriatna, S., Sukardi, R., and Rustandi, E., 1995. *Peta Geologi Lembar Samarinda, Kalimantan*, Pusat Penelitian dan Pengembangan Geologi. Bandung. Indonesia.

Tarantino, A. and De Col, E., 2008. Compaction behaviour of clay. *Géotechnique,* 58 (3), p.199-213. DOI: 10.1680/geot.2008.58.3.199.

Thurber, C.H. and Atre, S.R., 1993. Three-dimensional Vp/Vs variations along the Loma Prieta rupture zone. *Bulletin of the Seismological Society of America,* 83, p.717-736.

Torres, S.G., Pavoni, M., Barone, I., and Bast, A. 2024. Integration of Surface Wave Analysis with Electrical Resistivity and Seismic Refraction Tomography to Characterise Rock Glaciers. *NSG 2024 30th European Meeting of Environmental and Engineering Geophysics,* 2024 (1), p.1-5. European Association of Geoscientists and Engineers. DOI: 10.3997/2214-4609.202420183.

Tsai, V.C., Huber, C., and Dalton, C.A., 2023. Towards the geological parametrization of seismic tomography. *Geophysical Journal International,* 234 (2), p.1447-1462. DOI: 10.1093/gji/ggad140.

Uyanik, O., 2010. Compressional and shear-wave velocity measurements in unconsolidated topsoil and comparison of the results. *International Journal of the Physical Sciences,* 5 (7), p.1034-1039. DOI: 10.5897/IJPS.9000140.

Von Voigtlander, J., Clark, M.K., Zekkos, D., Greenwood, W.W., Anderson, S.P., Anderson, R.S., and Godt, J.W., 2018. Strong variation in weathering of layered rock maintains hillslope-scale strength under high precipitation. *Earth Surface Processes and Landforms,* 43 (6), p.1183-1194. DOI: 10.1002/esp.4290.

Waddell, P.J., Moyle, R.A., and Whiteley, R.J., 2010. Geotechnical verification of impact compaction. *WIT Transactions on Ecology and the Environment,* 141, p.73-85. DOI: 10.2495/BF100071.

White, D.J., 1989. Two-dimensional seismic refraction tomography. *Geophysical Journal International,* 97 (2), p.23-245.

Williams, R.A., Stephenson, W.J., and Odum, J.K., 2003. Comparison of P-and S-wave velocity profiles obtained from surface seismic refraction/reflection and downhole data. *Tectonophysics,* 368 (1-4), p.71-88. DOI: 10.1016/S0040-1951(03)00151-3.

Zelt, C.A. and Barton, P.J., 1998. Three-dimensional seismic refraction tomography: A comparison of two methods applied to data from the Faeroe Basin. *Journal of Geophysical Research: Solid Earth,* 103 (B4), p.7187-7210.